ORGANIC CHEMISTRY FRONTIERS

CHINESE CHEMICAL SOCIETY · SIOC · ROYAL SOCIETY OF CHEMISTRY

RESEARCH ARTICLE

View Article Online
View Journal | View Issue

Check for updates

Cite this: *Org. Chem. Front.*, 2025, **12**, 2011

Photoredox-catalyzed selective head-to-head reductive coupling of activated alkenes†

Shenhao Chen,‡[a] Zongchang Han,‡[b] Han-Shi Hu,[b] Jun Li[b] and Chanjuan Xi *[a,c]

Received 16th December 2024,
Accepted 23rd January 2025

DOI: 10.1039/d4qo02344g

rsc.li/frontiers-organic

Head-to-head reductive hydrodimerization of activated alkenes offers access to valuable bulk or fine chemicals such as adipates or adiponitrile as an intermediate for the industrial synthesis of nylon. We herein report a novel reaction to realize head-to-head reductive coupling of activated alkenes by a photo-induced Ir/PPh_3/H_2O system, providing smooth access to various adipate derivatives in high chemo- and regioselectivity. In this reaction, a [Ph_3P-OH] radical generated from a photoinduced interaction between H_2O and PPh_3 enables the PCET process with activated alkenes to form a C-centered radical at the β-position, which is rarely reported.

Dimerization of alkenes is a significant reaction for synthesizing essential intermediates for the production of bulk or fine chemicals.[1] Among them, selective head-to-head reductive dimerization of activated alkenes such as acrylates or acrylonitrile offers access to valuable adipates or adiponitrile as an intermediate for the industrial synthesis of nylon.[2] Early strategies for hydrodimerization of activated alkenes critically rely on utilizing stoichiometric metals as the reductant, which generates a large amount of metal wastes and limits the substrate scope due to unsatisfactory functional group tolerance.[3] Recently, transition-metal-catalyzed strategies have attracted much effort; however, the use of metal reductants is still necessary.[4] Meanwhile, a C=C bond remains in the dimerized products (Fig. 1a). Although electrolytic hydrodimerization of acrylonitrile to adiponitrile under aqueous conditions has been developed, this process is inapplicable to the synthesis of adipic derivatives (Fig. 1b).[5] Therefore, it is desirable to explore an environmentally friendly reduction mode for a head-to-head hydrodimerization of activated alkenes.

Recently, Studer's group developed a photocatalyzed Ir/PPh_3/H_2O system to realize hydrogenation of alkenes,[6] where the generated [Ph_3P-OH] radical provided a platform that mimics the reactivity of a 'free' hydrogen atom, which can be directly transferred to alkenes. The resulting H-adduct carbon radical shows the possibility to dimerize alkenes by radical coupling reaction.[7] Herein, we report a photoinduced Ir/PPh_3/H_2O system for a head-to-head (β,β-coupling) reductive dimerization of activated alkenes. In this reaction, the [Ph_3P-OH] radical is generated, enabling the proton coupled electron

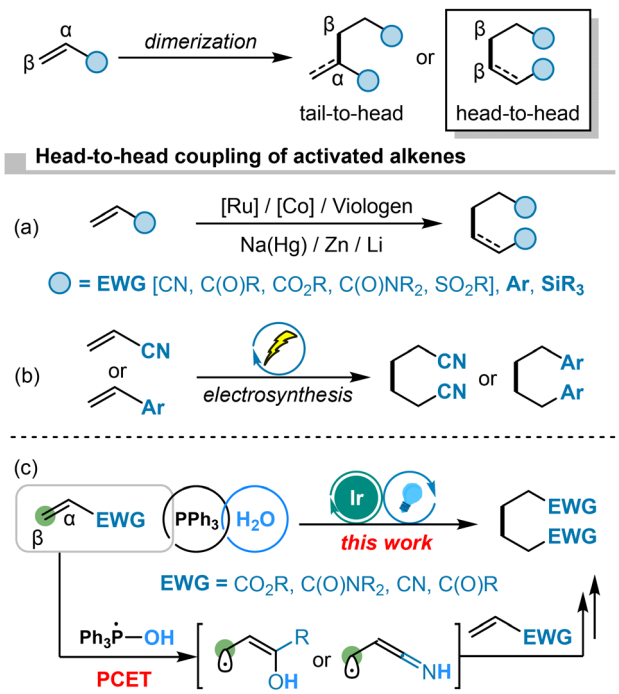

Fig. 1 Head-to-head dimerization of activated alkenes.

[a]MOE Key Laboratory of Bioorganic Phosphorus Chemistry & Chemical Biology, Department of Chemistry, Tsinghua University, Beijing 100084, China. E-mail: cjxi@tsinghua.edu.cn
[b]Department of Chemistry and Engineering Research Center of Advanced Rare-Earth Materials of Ministry of Education, Tsinghua University, Beijing 100084, China
[c]State Key Laboratory of Elemento-Organic Chemistry, Nankai University, Tianjin 300071, China

† Electronic supplementary information (ESI) available: General considerations, experimental procedures, mechanistic studies, analytical data of compounds, details of DFT calculations, DFT calculated energy and geometry coordinates, additional discussions and NMR spectra. See DOI: https://doi.org/10.1039/d4qo02344g

‡ These authors contributed equally to this work.

transfer (PCET) process[8] with activated alkenes, producing a nucleophilic β-C radical, followed by the Giese-type addition to the second molecule of activated alkenes, resulting in a reductive head-to-head coupling. Activated alkenes including acrylates, acrylamide, acrylonitrile and vinyl ketones with α or β substituents are well-tolerated in this conversion, providing approaches to various valuable adipate derivatives, adiponitrile and 1,6-diones (Fig. 1c).

We initiated the study by employing *tert*-butyl acrylate **1a** as the substrate, $Ir[dF(CF_3)ppy]_2(dtbbpy)PF_6$ as the photocatalyst and PPh_3 as the reductant. After irradiation under a N_2 atmosphere for 21 hours, di-*tert*-butyl adipate **2a** as the head-to-head coupling product was successfully obtained in 77% yield (Table 1, entry 1). Notably, the tail-to-head coupling (α,β-coupling) product was not observed, showing high regioselectivity of this reaction. Reducing the volume of acetonitrile (CH_3CN) to 1 mL resulted in an obvious loss of yield, while increasing the volume of CH_3CN to 3 mL did not affect the reaction, indicating that dilute conditions were more suitable (entries 2 and 3). Changing CH_3CN to dimethylformamide (DMF) or dimethyl sulfoxide (DMSO) resulted in a messy mixture with only a trace amount of **2a** detected (entries 4 and 5). To accelerate the reaction, excess PPh_3 was necessary, but a larger excess amount also led to the hydrogenation of alkenes as the side reaction, and 1.0 equivalent of PPh_3 was found to be the best amount (entries 6 and 7). The decrease in the amount of water resulted in a slight drop of the yield of product **2a**, and 21 hours were enough for this reaction (entries 8–11). The reaction was inhibited without either photocatalyst, PPh_3, H_2O or light irradiation (entry 12).

Table 1 Optimization of the reaction conditions[a]

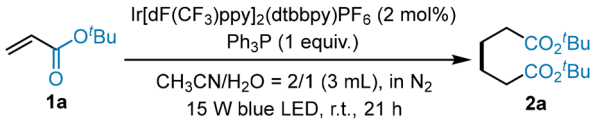

Entry	Verified conditions	Yield[b] (%)
1	Standard conditions	77 (72)
2	Solvent: CH_3CN (1 mL)	40
3	Solvent: CH_3CN (3 mL)	77
4	Solvent: DMF (2 mL)	Trace
5	Solvent: DMSO (2 mL)	Trace
6	Amount PPh_3: 2.0 equiv.	70
7	Amount PPh_3: 0.5 equiv.	48
8	Volume of H_2O: 0.50 mL	68
9	Volume of H_2O: 0.15 mL	61
10	Reaction time: 12 h	30
11	Reaction time: 48 h	78
12	Without [Ir] or PPh_3 or H_2O or light irradiation	N.D.

[a] Standard conditions: *tert*-butyl acrylate **1a** (0.2 mmol), $Ir[dF(CF_3)ppy]_2(dtbbpy)PF_6$ (2.0 mol%), PPh_3 (1.0 equiv.), H_2O (1.0 mL) and CH_3CN (2.0 mL), under a N_2 atmosphere, 15 W blue LEDs, 21 h irradiation at room temperature. [b] Yields determined by ^1H NMR using CH_2Br_2 as the internal standard, isolated yield given in parenthesis. N.D.: not detected.

With the optimized conditions in hand, various activated alkenes were tested to explore the substrate scope of this reductive coupling system. The representative results are shown in Fig. 2. Terminal acrylate with a *tert*-butyl group on the ester side (**1a**) was tolerated and the corresponding product (**2a**) was isolated in 72% yield. Acrylates with α-methyl group (**1b**) were capable of the conversion, while epoxy group and chloride at the ester part were also tolerated and generated products (**2c** and **2d**) in excellent yield, respectively. α-Fluoride (**1e**) and α-phenyl acrylate (**1f**) were also suitable for the conversion to afford hydrodimerized products (**2e–2f**) in 76% and 33% yields, respectively. The lower yield of **2f** can be attributed to the steric hindrance and hydrogenation of the vinyl group as the by-product. γ-Lactone with an exocyclic C=C bond also completed this transformation smoothly to produce **2g** in moderate yield. Moreover, β-substituted and α,β-disubstituted acrylates performed well with two ester groups on substrates (**1h–1i**). The benzylic and phenyl acrylates (**1j–1k**) were tolerated, but suffered from the hydrolysis of the ester group, resulting in poorer yields [for details see Fig. S3 in the ESI†]. In addition, acrylonitrile could be converted into adiponitrile

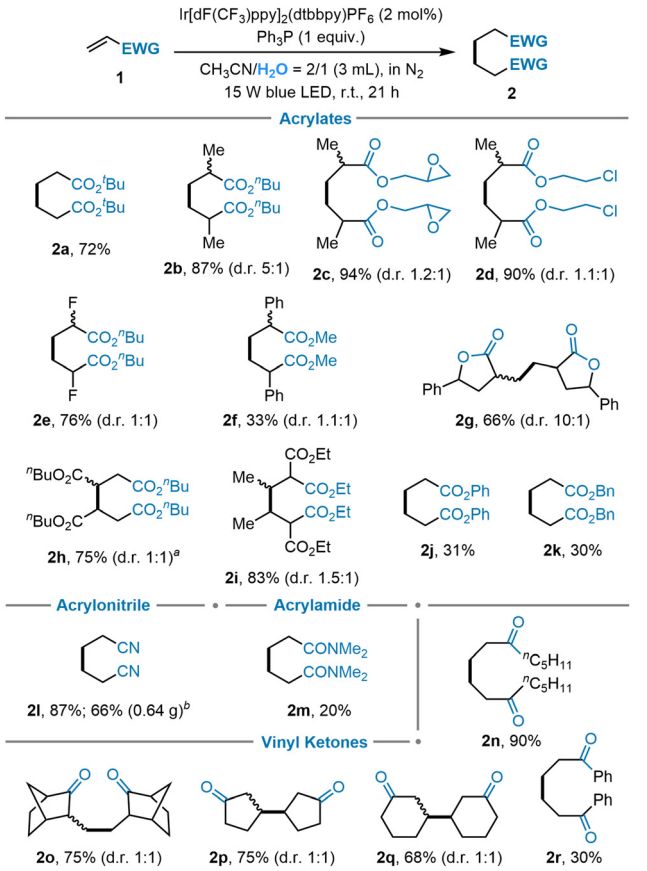

Fig. 2 Substrate scope of the reductive coupling system. Standard conditions: activated alkene 1 (0.2 mmol), $Ir[dF(CF_3)ppy]_2(dtbbpy)PF_6$ (2.0 mol%), PPh_3 (1.0 equiv.), H_2O (1.0 mL), CH_3CN (2.0 mL), under a N_2 atmosphere, 15 W blue LEDs, 21 h irradiation at room temperature. [a](*E*)-Dibutyl succinate as the substrate. [b]18 mmol scale.

2l in high yield, and the scale-up reaction (18 mmol) proceeded smoothly to produce **2l** in moderate yield (0.64 g, 66%). Acrylamide **1m** was also tolerated; however, it resulted in poor chemoselectivity due to the competitive hydrogenation of the C=C bond as a byproduct. Vinyl ketones were also applicable in this reaction, including linear ketones (**1n**), ketone with an exocyclic C=C bond on a norbornene skeleton (**1o**), and ketones with an endocyclic C=C bond in five/six-membered rings (**1p–1q**), to give the corresponding products in high yields. Phenyl vinyl ketone could be transformed into product **2r**, but the hydrogenation of the carbonyl group[9] interfered with the reaction. Propargyl ester with a carbon–carbon triple bond was also suitable for this conversion with 2.0 equivalents of PPh_3 to produce head-to-head coupling product **2a** in 33% yield.

To gain insight into the reaction process, several experiments were designed. The reaction was completely inhibited by the addition of 3.5 equivalents of 2,2,6,6-tetramethyl-1-piperinedinyloxy (TEMPO) (Fig. 3A-(i)), revealing the involvement of a potential radical process. When employing cyclopropyl group at the α-position of acrylate **3**, the reductive coupling reaction was inhibited, and the acrylate **3** underwent a ring-opening process to generate linear product **4** by the hydrogenation instead (Fig. 3A-(ii)), which further indicates the radical process in this reaction. To verify whether the reaction proceeded *via* a [2 + 2] cycloaddition and direct hydrogenation of the cyclobutyl motif, **1a** was first exposed to light irradiation and products **5** with a cyclobutene skeleton were not detected in the presence/absence of the photocatalyst. Then, 1,2-cyclobutanedioicates (***trans*-5** and ***cis*-6**) were also tested under standard conditions and it was found that the reaction did not proceed and the starting materials remained. These results excluded the possibility of cyclobutanedioicate as the intermediate (Fig. 3B). When replacing H_2O with D_2O under the standard conditions, the deuterium ratio at the α-position in ***d*-2a** reached 77/23, indicating that water was the hydrogen source in this reaction. Additionally, an unexpected deuterium ratio of 15/85 at the β-position of ***d*-2a** was observed, suggesting the possibility of the formation of a β-activated intermediate in this reaction (Fig. 3C).

Stern–Volmer experiments demonstrated that PPh_3 exhibited the strongest fluorescence quenching ability of the iridium-based catalyst, while acrylate **1a** and acrylonitrile **1l** barely affected the fluorescence strength of the photocatalyst. Vinyl ketone **1n** presents a degree of quenching ability, but it is weaker than that of PPh_3. The quenching ability of PPh_3 changed slightly in the presence of H_2O, implying a low possibility of interaction between PPh_3 and H_2O in the quenching process, indicating that PPh_3 was the dominant quencher of the photocatalyst (Fig. 4).

In order to further explain the anomalous selectivity, computational studies have been carried out. All quantum chemical calculations were carried out using Gaussian 16B and ORCA 6.0, while all crossing points were found using KST48 (see section 9.1 in the ESI for details†).[10] The Gibbs free energy diagram of the stepwise pathway is shown in Fig. 5. The

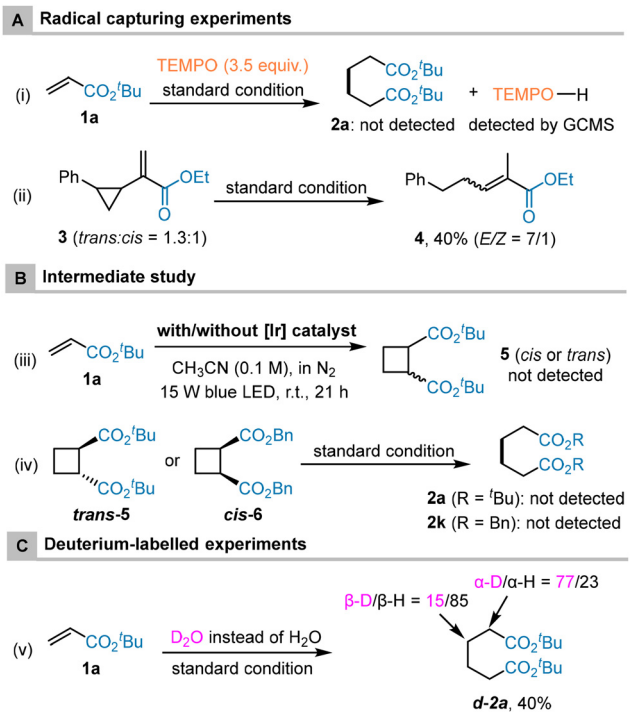

Fig. 3 Experiments of the mechanistic study.

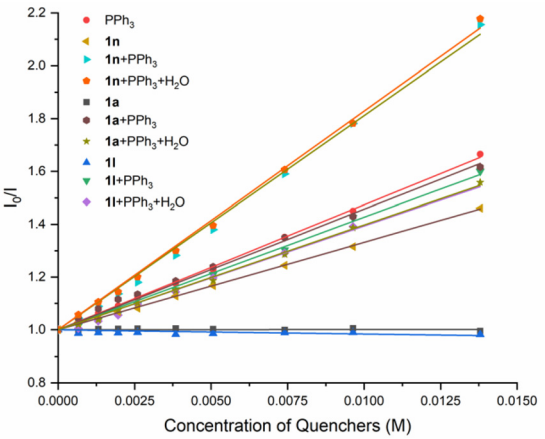

Structure	Quencher	K_{SV} (M^{-1})
-	PPh_3	47.4
1n	**1n**	33.2
	1n +Ph_3P	81.1
	1n +Ph_3P + H_2O	82.9
1a	**1a**	0.102
	1a +Ph_3P	45.7
	1a +Ph_3P + H_2O	39.7
1l	**1l**	-1.61
	1l +Ph_3P	42.7
	1l +Ph_3P + H_2O	39.3

Fig. 4 Fluorescence quenching experiments.

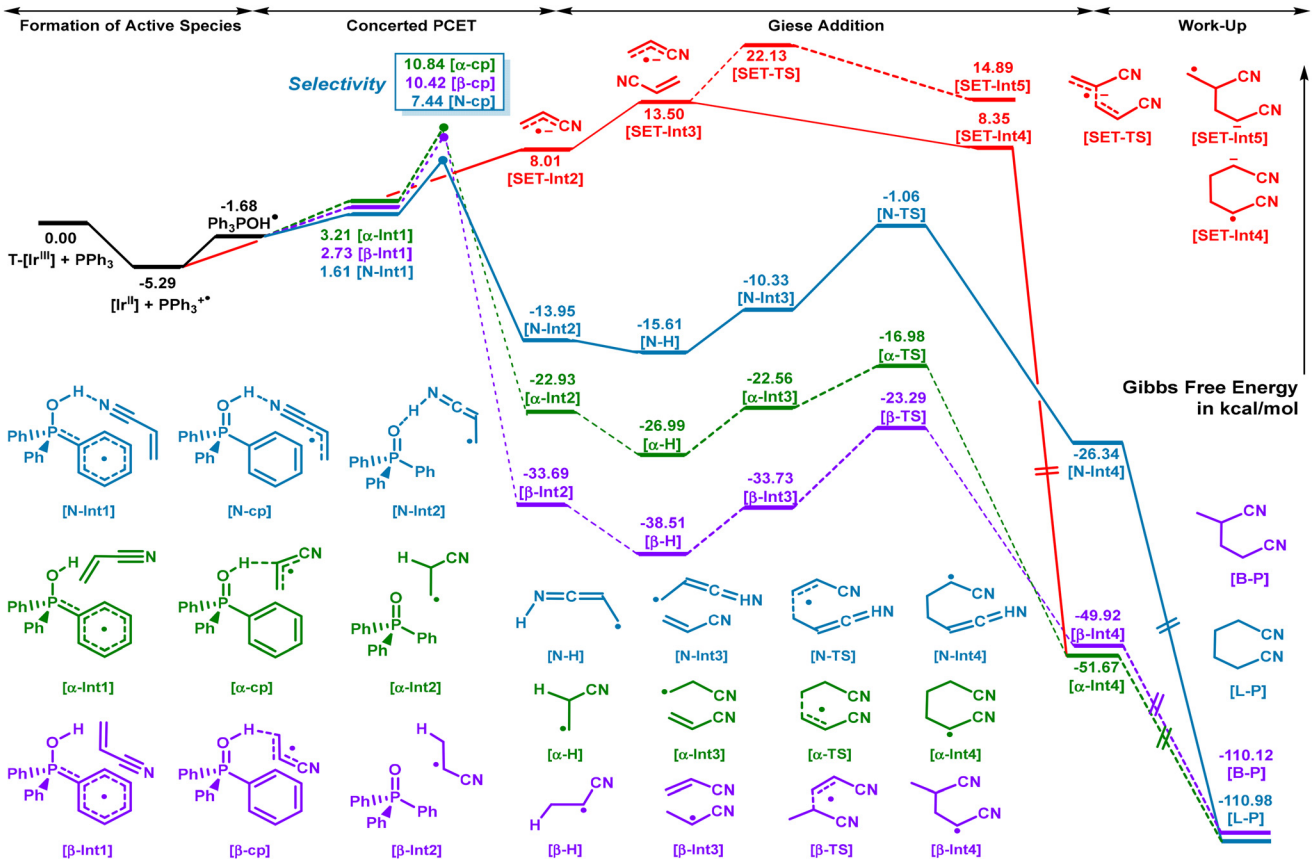

Fig. 5 Gibbs free energy diagram of the reaction with acrylonitrile as substrates. T = Triplet, L = Linear, B = Branched, Int = Intermediate, TS = Transition State, cp = crossing point, P = Product, SET = Single Electron Transfer; α, β and N are sites of hydrogen transfer; see section 9.4 in the ESI† for additional details.

reaction is initiated by a single electron transfer (SET) process between the photocatalyst (**T-[Ir$^+$]**) in the triplet state and Ph_3P, followed by interaction with H_2O to form the [Ph_3P-OH] radical.[6,9,11] Calculations show that the generation of the [Ph_3P-OH] radical [$E_{1/2}(Ph_3POH^+/Ph_3POH^\bullet) = -1.75$ V *vs.* SHE] is energetically permissive, and the following reactions with three sites of acrylonitrile (N, α-C and β-C) are concerted PCET processes. The lowest total Gibbs free energy barrier is 12.73 kcal mol^{-1} for the crossing point to **[N-cp]**, while that of **[β-cp]** and **[α-cp]** is about 3.0 kcal mol^{-1} and 3.4 kcal mol^{-1} higher respectively, leading to an anomalous selectivity. Time-scale reactions with H_2O/D_2O showed a primary isotope effect ($k_H/k_D > 5$, see Fig. S4†), indicating the possibility of a concerted PCET step as the rate determining step. The structures then dissociate into Ph_3PO and three types of C-centered radicals respectively, which could undergo Giese addition to another acrylonitrile molecule. Although the barrier for the **[N–H]** is slightly higher than the other two processes, the global barrier for this pathway is more favorable. The following spontaneous reduction and protonation processes produce the linear structure as the major product. Another possible pathway is the direct reduction of acrylonitrile by **[Ir^{II}]** to form the acrylonitrile radical anion **[SET-Int2]** and then the pre-complex **[SET-Int3]** with an 18.79 kcal mol^{-1} barrier, followed by barrierless Giese addition to give the linear product. The higher energies of **[SET-TS]** and **[SET-Int5]** inhibit the formation of the branched product. This SET pathway is likely to be a side pathway for the generation of the linear product (see section 9.4 in the ESI for details†).

The effect of weak interactions in the concerted PCET process was also studied, indicating that the hydrogen bonding between the [Ph_3P-OH] radical and activated alkenes accounts for the anomalous selectivity (see detailed IGMH and ETS-NOCV analysis[12] in Fig. S7 of the ESI†). The reaction coordinates of the two PES before and after electron transfer were defined by the species before and after hydrogen transfer, and the crossing point was approximated by a straight line connecting the two surfaces. When neglecting the hydrogen bonding effect in the concerted PCET process, the crossing point energy of **[β-cp]** is lower than **[N-cp]′**, leading to non-existent branched products (Fig. 6a). When the hydrogen bonding effect is considered, both the reactant and the product experience a significant energy decrease, resulting in a lower crossing point energy of **[N-cp]**, thus explaining the selective generation of the linear product (Fig. 6b). The possibility of stepwise ET–PT (electron transfer–proton transfer) and concerted HAT (hydrogen atom transfer) instead of a concerted PCET process is also ruled out (see Fig. S8 of the ESI†).

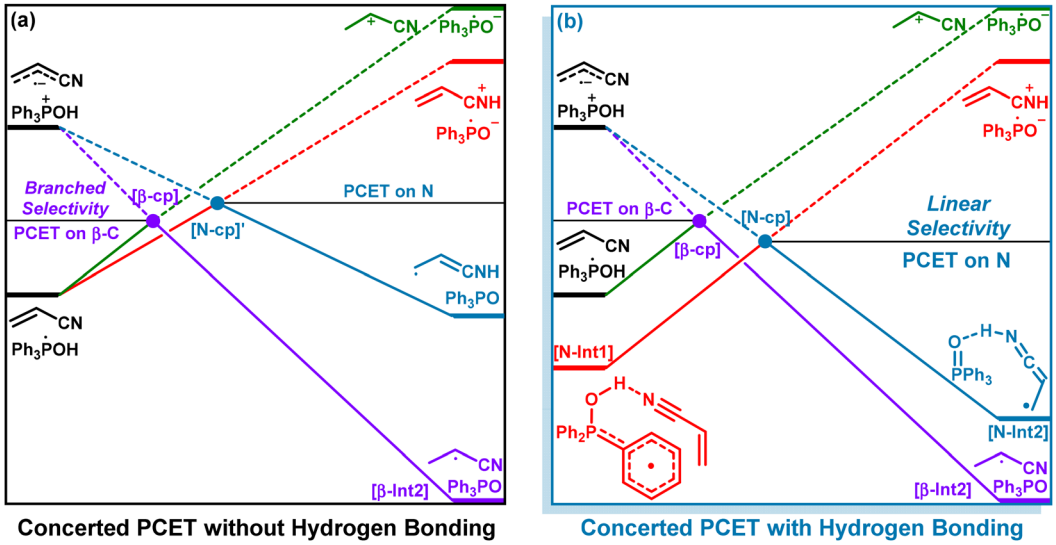

Fig. 6 Mechanism diagram of PCET to acrylonitrile.

A plausible mechanism is proposed and shown in Fig. 7. The reaction is initiated by photoinduced single electron transfer (SET) from PPh_3 to T-[Ir^{III}] in the excited state, forming a PPh_3 radical cation ($PPh_3^{\cdot+}$), which could accept nucleophilic H_2O and deprotonate to afford the [Ph_3P-OH] radical. The [Ph_3P-OH] radical could undergo a concerted PCET process with substrates (acrylonitrile as an example), and the energy barrier for PCET *via* the crossing point **[N-cp]** (12.73 kcal mol^{-1}) is lower than that of **[α-cp]** (16.13 kcal mol^{-1}) and **[β-cp]** (15.71 kcal mol^{-1}), which results in the selective formation of the radical **[N–H]** (**A**). **A** then undergoes Giese addition to a second molecule of acrylonitrile to generate the radical **[N-Int4]**, which could receive electrons from Ir^{II}, followed by tautomerization and protonation to produce the head-to-head coupling product. Even though the radical **[β-H]** (**C**) from the ET–PT or HAT process is thermodynamically more stable than **A**, the formation of **C** is not favored because it leads to the head-to-tail coupling product that is not detected.

Conclusions

In summary, we have disclosed a photoinduced strategy for the head-to-head reductive coupling of activated alkenes, producing various adipate derivatives, adiponitrile and 1,6-diones with high chemo- and regio-selectivity with water as the hydrogen source. In this reaction, the [Ph_3P-OH] radical is generated from a photoinduced interaction between H_2O and PPh_3, followed by a PCET process with activated alkenes to form a nucleophilic radical at the β-position. The β-C activation strategy provides insights into different regioselectivity reactions

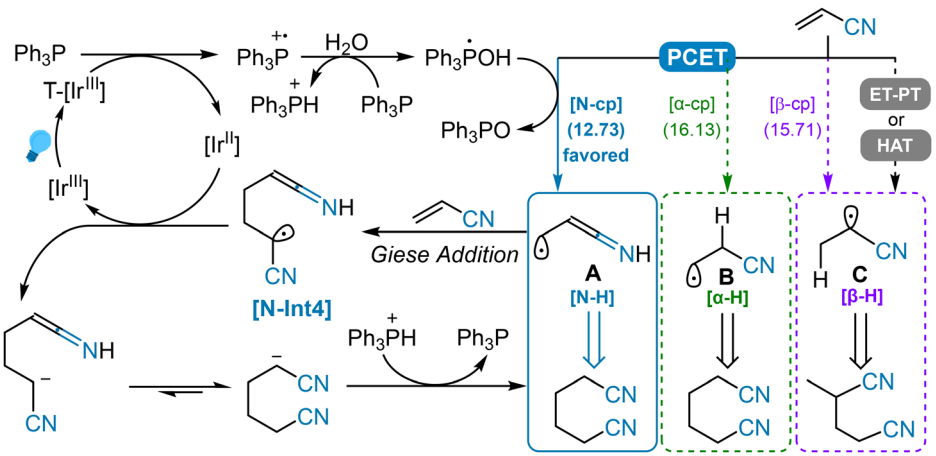

Fig. 7 Proposed mechanism for the reductive coupling of activated alkenes (total Gibbs free energy barrier for the PCET process is given in parenthesis, kcal mol^{-1}).

with activated alkenes, building new synthetic methods through radical processes.

Author contributions

The manuscript was conceived and written through contributions from all authors. All authors have approved the final version of the manuscript.

Data availability

Data including experimental procedures, characteristic details for both new compounds and known compounds synthesized by a new method, copies of ^{1}H, ^{13}C, and ^{19}F NMR spectra of new starting materials and all products as well as details of DFT calculations, DFT calculated energy and geometry coordinates are available in the ESI.†

Conflicts of interest

There are no conflicts to declare.

Acknowledgements

We are grateful for financial support from the National Natural Science Foundation of China (22371159 and 22071134). We also thank Yumiao Ma from BSJ Institute for the enlightening discussion of the reaction mechanism and the equipment for computational studies.

References

1 (*a*) C. Janiak, Metallocene and related catalysts for olefin, alkyne and silane dimerization and oligomerization, *Coord. Chem. Rev.*, 2006, **250**, 66–94; (*b*) M. Jeganmohan and C.-H. Cheng, Cobalt- and Nickel-Catalyzed Regio- and Stereoselective Reductive Coupling of Alkynes, Allenes, and Alkenes with Alkenes, *Chem. – Eur. J.*, 2008, **14**, 10876–10886; (*c*) M. Hirano and S. Komiya, Oxidative coupling reactions at ruthenium(0) and their applications to catalytic homo- and cross-dimerizations, *Coord. Chem. Rev.*, 2016, **314**, 182–200; (*d*) M. Hirano, Recent Advances in the Catalytic Linear Cross-Dimerizations, *ACS Catal.*, 2019, **9**, 1408–1430; (*e*) Q. Liang, K. Hayashi and D. Song, Catalytic Alkyne Dimerization without Noble Metals, *ACS Catal.*, 2020, **10**, 4895–4905.

2 (*a*) W. Yan, G. Zhang, J. Wang, M. Liu, Y. Sun, Z. Zhou, W. Zhang, S. Zhang, X. Xu, J. Shen and X. Jin, Recent Progress in Adipic Acid Synthesis Over Heterogeneous Catalysts, *Front. Chem.*, 2020, **8**, 185; (*b*) J. Rios, J. Lebeau, T. Yang, S. Li and M. D. Lynch, A critical review on the progress and challenges to a more sustainable, cost competitive synthesis of adipic acid, *Green Chem.*, 2021, **23**, 3172–3190; (*c*) M. Lang and H. Li, Sustainable Routes for the Synthesis of Renewable Adipic Acid from Biomass Derivatives, *ChemSusChem*, 2022, **15**, e202101531.

3 (*a*) F. Matsuda, Reductive coupling of olefinic compounds by an alkali metal amalgam, *Tetrahedron Lett.*, 1966, **7**, 6192–6197; (*b*) T. Endo, K. Ageishi and M. Okawara, Reduction of acrylonitrile in the presence of viologen derivatives, *J. Org. Chem.*, 1986, **51**, 4309–4310.

4 (*a*) C.-C. Wang, P.-S. Lin and C.-H. Cheng, Cobalt-catalyzed dimerization of alkenes, *Tetrahedron Lett.*, 2004, **45**, 6203–6206; (*b*) K. Kashiwagi, R. Sugise, T. Shimakawa and T. Matuura, Improvement of Catalyst Activity in the Ru-catalyzed Dimerization of Acrylonitrile by Using Diphenyl Ether as a Solvent, *Chem. Lett.*, 2007, **36**, 1384–1385; (*c*) P. K. Maity and J. A. Tunge, Assisted Tandem Catalytic Conversion of Acrylates into Adipic Esters, *ChemCatChem*, 2018, **10**, 3419–3423; (*d*) C. Ren, G. Ji, X. Li and J. Zhang, Direct Synthesis of Adipic Esters and Adiponitrile via Photoassisted Cobalt-Catalyzed Alkene Hydrodimerization, *Chem. – Eur. J.*, 2022, **28**, e202201442; (*e*) Y. Jiang and H. Yorimitsu, Taming Highly Unstable Radical Anions and 1,4-Organodilithiums by Flow Microreactors: Controlled Reductive Dimerization of Styrenes, *JACS Au*, 2022, **2**, 2514–2521.

5 (*a*) V. Klimov and A. Tomilov, Effect of the structure of quaternary ammonium-salts on the cathodic hydrodimerization of acrylonitrile, *Russ. J. Appl. Chem.*, 1993, **66**, 898–901; (*b*) S. Wu, J. Cheng, Y. Xiang, Y. Tu, X. Huang and Z. Wei, Electrochemical semi-hydrogenation of adiponitrile over copper nanowires as a key step for the green synthesis of nylon-6, *Chem. Sci.*, 2024, **15**, 11521–11527; (*c*) S. Ning, L. Zheng, Y. Bai, S. Wang, S. Wang, L. Shi, Q. Gao, X. Che, Z. Zhang and J. Xiang, Highly selective electroreductive linear dimerization of electron-deficient vinylarenes, *Tetrahedron*, 2021, **102**, 132535.

6 J. Zhang, C. Mück-Lichtenfeld and A. Studer, Photocatalytic phosphine-mediated water activation for radical hydrogenation, *Nature*, 2023, **619**, 506–513.

7 (*a*) A. L. Gant Kanegusuku and J. L. Roizen, Recent Advances in Photoredox-Mediated Radical Conjugate Addition Reactions: An Expanding Toolkit for the Giese Reaction, *Angew. Chem., Int. Ed.*, 2021, **60**, 21116–21149; (*b*) Y. Roh, H.-Y. Jang, V. Lynch, N. L. Bauld and M. J. Krische, Anion Radical Chain Cycloaddition of Tethered Enones: Intramolecular Cyclobutanation and Diels–Alder Cycloaddition, *Org. Lett.*, 2002, **4**, 611–613.

8 (*a*) J. J. Concepcion, M. K. Brennaman, J. R. Deyton, N. V. Lebedeva, M. D. E. Forbes, J. M. Papanikolas and T. J. Meyer, Excited-State Quenching by Proton-Coupled Electron Transfer, *J. Am. Chem. Soc.*, 2007, **129**, 6968–6969; (*b*) M. H. V. Huynh and T. J. Meyer, Proton-Coupled Electron Transfer, *Chem. Rev.*, 2007, **107**, 5004–5064; (*c*) E. C. Gentry and R. R. Knowles, Synthetic Applications of Proton-Coupled Electron Transfer, *Acc. Chem. Res.*, 2016, **49**, 1546–1556.

9 S. Chen and C. Xi, Photoinduced catalytical reduction of carbonyl compounds using water as a hydrogen source, *Org. Chem. Front.*, 2024, **11**, 5415–5421.

10 (*a*) M. Frisch, G. Trucks, H. B. Schlegel, G. Scuseria, M. Robb, J. Cheeseman, G. Scalmani, V. Barone, G. Petersson and H. Nakatsuji, *Gaussian 16*, Gaussian, Inc, Wallingford, CT, 2016; (*b*) R. Colle and O. Salvetti, Approximate calculation of the correlation energy for the closed and open shells, *Theor. Chim. Acta*, 1979, **53**, 55–63; (*c*) F. Weigend and R. Ahlrichs, Balanced basis sets of split valence, triple zeta valence and quadruple zeta valence quality for H to Rn: Design and assessment of accuracy, *Phys. Chem. Chem. Phys.*, 2005, **7**, 3297–3305; (*d*) F. Weigend, Accurate Coulomb-fitting basis sets for H to Rn, *Phys. Chem. Chem. Phys.*, 2006, **8**, 1057–1065; (*e*) A. Hellweg, C. Hättig, S. Höfener and W. Klopper, Optimized accurate auxiliary basis sets for RI-MP2 and RI-CC2 calculations for the atoms Rb to Rn, *Theor. Chem. Acc.*, 2007, **117**, 587–597; (*f*) J.-D. Chai and M. Head-Gordon, Long-range corrected hybrid density functionals with damped atom–atom dispersion corrections, *Phys. Chem. Chem. Phys.*, 2008, **10**, 6615–6620; (*g*) A. V. Marenich, C. J. Cramer and D. G. Truhlar, Universal Solvation Model Based on Solute Electron Density and on a Continuum Model of the Solvent Defined by the Bulk Dielectric Constant and Atomic Surface Tensions, *J. Phys. Chem. B*, 2009, **113**, 6378–6396; (*h*) F. Neese, The ORCA program system, *Wiley Interdiscip. Rev.: Comput. Mol. Sci.*, 2012, **2**, 73–78; (*i*) Y. Ma, KST48: A Powerful Tool for MECP location, **https://github.com/RimoAccelerator/KST48**, (accessed on December 16, 2024); (*j*) Y. Ma and A. A. Hussein, Formal Pericyclic-Coupled Electron Transfer: I. Stepwise Formal Diels-Alder Cycloaddition Enabled by Addition-Coupled Electron Transfer, *ChemistrySelect*, 2022, **7**, e202202354; (*k*) F. Neese, Software update: The ORCA program system—Version 5.0, *Wiley Interdiscip. Rev.: Comput. Mol. Sci.*, 2022, **12**, e1606; (*l*) F. Neese, The SHARK integral generation and digestion system, *J. Comput. Chem.*, 2023, **44**, 381–396; (*m*) C. Angeli, R. Cimiraglia, S. Evangelisti, T. Leininger and J.-P. Malrieu, Introduction of n-electron valence states for multireference perturbation theory, *J. Chem. Phys.*, 2001, **114**, 10252–10264.

11 (*a*) M. Zhang, X.-A. Yuan, C. Zhu and J. Xie, Deoxygenative Deuteration of Carboxylic Acids with D_2O, *Angew. Chem., Int. Ed.*, 2019, **58**, 312–316; (*b*) W.-J. Kang, Y. Pan, A. Ding and H. Guo, Organophotocatalytic Alkene Reduction Using Water as a Hydrogen Donor, *Org. Lett.*, 2023, **25**, 7633–7638; (*c*) Z.-Z. Xie, Y. Zheng, Z.-H. Liao, C.-P. Yuan, M.-Z. Li, K.-Y. Deng, H.-Y. Xiang, K. Chen and H. Yang, Photoredox-catalyzed hydrogenation of alkenes assisted by an in situ generated $PPh_3(OH)$ radical and acetic acid, *Org. Chem. Front.*, 2024, **11**, 4187–4193; (*d*) Z.-Z. Xie, Z.-H. Liao, Y. Zheng, C.-P. Yuan, J.-P. Guan, M.-Z. Li, K.-Y. Deng, H.-Y. Xiang, K. Chen and H. Yang, Photoredox-Catalyzed Selective α-Scission of PR_3–OH Radicals to Access Hydroalkylation of Alkenes, *Org. Lett.*, 2023, **25**, 9014–9019.

12 (*a*) W. Humphrey, A. Dalke and K. Schulten, VMD: Visual molecular dynamics, *J. Mol. Graphics*, 1996, **14**, 33–38; (*b*) M. P. Mitoraj, A. Michalak and T. Ziegler, A Combined Charge and Energy Decomposition Scheme for Bond Analysis, *J. Chem. Theory Comput.*, 2009, **5**, 962–975; (*c*) T. Lu and F. Chen, Multiwfn: A multifunctional wavefunction analyzer, *J. Comput. Chem.*, 2012, **33**, 580–592; (*d*) T. Lu and Q. Chen, Independent gradient model based on Hirshfeld partition: A new method for visual study of interactions in chemical systems, *J. Comput. Chem.*, 2022, **43**, 539–555.